Title

Cdc45 (cell division cycle protein 45) guards the gate of the Eukaryote Replisome helicase stabilizing leading strand engagement

Journal

Proceedings of the National Academy of Sciences of the United States of America, 112(3)

ISSN

0027-8424

Authors

Petojevic, Tatjana
Pesavento, James J
Costa, Alessandro
et al.

Publication Date

2015-01-20

DOI

10.1073/pnas.1422003112

Peer reviewed

Cdc45 (cell division cycle protein 45) guards the gate of the Eukaryote Replisome helicase stabilizing leading strand engagement

Tatjana Petojevic[a,b,1], James J. Pesavento[a,1], Alessandro Costa[c], Jingdan Liang[a], Zhijun Wang[a], James M. Berger[d,2], and Michael R. Botchan[a,2]

[a]Department of Molecular and Cell Biology, Division of Biochemistry and Molecular Biology, University of California, Berkeley, CA 94720; [b]Department of Biology, Chemistry and Pharmacy, Institute of Chemistry and Biochemistry, Freie Universität Berlin, 14195 Berlin, Germany; [c]Clare Hall Laboratories, London Research Institute, South Mimms, Herts EN6 3LD, United Kingdom; and [d]Department of Biophysics and Biophysical Chemistry, School of Medicine, Johns Hopkins University, Baltimore, MD 21205

Contributed by Michael R. Botchan, December 10, 2014 (sent for review November 17, 2014; reviewed by Michael O'Donnell and Bruce Stillman)

DNA replication licensing is now understood to be the pathway that leads to the assembly of double hexamers of minichromosome maintenance (Mcm2–7) at origin sites. Cell division control protein 45 (Cdc45) and GINS proteins activate the latent Mcm2–7 helicase by inducing allosteric changes through binding, forming a Cdc45/Mcm2-7/GINS (CMG) complex that is competent to unwind duplex DNA. The CMG has an active gate between subunits Mcm2 and Mcm5 that opens and closes in response to nucleotide binding. The consequences of inappropriate Mcm2/5 gate actuation and the role of a side channel formed between GINS/Cdc45 and the outer edge of the Mcm2–7 ring for unwinding have remained unexplored. Here we uncover a novel function for Cdc45. Cross-linking studies trace the path of the DNA with the CMG complex at a fork junction between duplex and single strands with the bound CMG in an open or closed gate conformation. In the closed state, the lagging strand does not pass through the side channel, but in the open state, the leading strand surprisingly interacts with Cdc45. Mutations in the recombination protein J fold of Cdc45 that ablate this interaction diminish helicase activity. These data indicate that Cdc45 serves as a shield to guard against occasional slippage of the leading strand from the core channel.

DNA replication | CMG helicase | Cdc45 | RecJ fold | Mcm2/5 gate

Chromosomal DNA replication begins with the separation of the complementary strands of the duplex. Following this melting step, helicases continuously separate the paired strands, exposing the template for enzymatic synthesis. For eukaryotic DNA replication, a growing body of work suggests that the initial DNA melting step involves an enzymatic conversion of a double hexamer of the minichromosome maintenance (Mcm2–7) complex into an active helicase, with hexamer separation forming two forks moving in opposite directions (1). The molecular mechanisms and a complete list of the factors that work to achieve melting and the topological conversion of double to single strand are still unknown, but both Cdc45 and the GINS complex are present at the time of melting (2) and are critical components of an activated Mcm2–7 helicase (3–6). Understanding the initiation process requires studies focused on the various transitions accessed by Mcm2–7 proteins and defining what roles the GINS and Cdc45 may play in the melting and unwinding processes.

The CMG helicase characterized in vitro in *Drosophila* and humans contains a single Cdc45 protein, a single hetero-hexameric Mcm2–7, and a tetrameric GINS complex (3–7). Mcm2–7 acts as the motor that drives helicase activity; however, for metazoans, only when the Mcm2–7 complex is associated with Cdc45 and GINS do significant helicase, ATPase, and DNA binding activities follow (4). The two Mcm2–7 complexes are first loaded to DNA by mechanisms that appear to retain certain parallels to the processes used for loading sliding processivity clamps onto DNA. The endpoint of loading results in the deposition of a duplex DNA that runs through the central channel of an MCM double hexamer. Although topologically linked to DNA, the associated Mcm2–7 double hexamer appears to only weakly engage the duplex, as it can slide off a linearized segment in the absence of a blocking barrier (8, 9).

Following double-hexamer formation, a transition is thought to occur whereby the lagging strand exits the central channel of the MCM ring and the leading strand remains in the central channel. Evidence for this transition follows from biochemical studies showing that the replication fork can bypass a roadblock on the lagging (5′–3′) but not the leading (3′–5′) strand (10) and that the CMG can only bind single-stranded DNA presented at a fork (4). Similarly, both biochemical and structural studies with the homologous archaeal MCM helicases have revealed that the leading strand must pass through the central pore of the helicase, whereas the lagging strand takes an external path (11–14).

Our focus to compare the structure and function of the CMG with Mcm2–7 has been motivated by two considerations. First, understanding the allosteric induction of helicase activity accomplished by the GINS and Cdc45 proteins should inform the mechanism for initiation, the notion here being that the first melting step might be coupled to the formation of the active helicase. Second, the active CMG helicase coordinates the assembly of key proteins for DNA strand synthesis—such as Ctf4

Significance

Cell division control protein 45 (Cdc45), a RecJ homologue, is essential in all eukaryotes. Cdc45 functions with the replisome CMG helicase where minichromosome maintenance (Mcm2–7) proteins provide motor activity for unwinding duplex during replication. We report that the dynamic gate between Mcm subunits 2 and 5, which is essential for the initial loading of the motor, may be an Achilles heel because the leading strand may slip from its central channel in an open gate state. Studies show that the side channel formed by the Cdc45 and GINS works as a trap and guards this gate; the Recombination protein J fold is key for this activity. We propose that this new function for Cdc45 will be important for fork integrity during the S-phase in response to double-strand breaks or replication stress.

Author contributions: T.P., J.J.P., A.C., J.M.B., and M.R.B. designed research; T.P., J.J.P., and A.C. performed research; J.L. and Z.W. contributed new reagents/analytic tools; T.P., J.J.P., A.C., J.M.B., and M.R.B. analyzed data; and T.P., J.M.B., and M.R.B. wrote the paper.

Reviewers: M.O., Rockefeller University; and B.S., Cold Spring Harbor Laboratory.

The authors declare no conflict of interest.

[1]T.P. and J.J.P. contributed equally to this work.

[2]To whom correspondence may be addressed. Email: mbotchan@berkeley.edu or jmberger@jhmi.edu.

This article contains supporting information online at www.pnas.org/lookup/suppl/doi:10.1073/pnas.1422003112/-/DCSupplemental.

(15), Mcm10 (16), and polε (17)—implying that structural transitions in the Mcm2–7 complex affected by the GINS and Cdc45 may assist in recruitment and function of multiple activities of the replisome. How the Mcm2–7 proteins might influence these interactions or how leading and lagging strand synthesis might be coordinated with unwinding are unknown. Thus, the path of both the leading and lagging strands and the functions of the nonmotor proteins in the complex are important for a more complete picture of the eukaryotic replisome.

In previous studies, we have shown that in the CMG, GINS and Cdc45 bridge a gap between the Mcm2 and Mcm5 subunits, and that when a nucleotide is bound, these interactions seal off the interior channel, creating a topologically segregated second channel to the side of the central axis of the Mcm2–7 ring (18). In the apo state, interactions between Mcm2 and Mcm5 change, creating an opening between the subunits that renders the space of the interior channel contiguous with the external side channel. This discontinuity between Mcm2 and Mcm5 was first described biochemically in the yeast Mcm2–7 complex (19) and has been called a "gate," as opening between the subunits at this position is crucial for loading to substrates in biochemical assays. For the CMG, given that amino acids in Mcm5 and Mcm2 are both required for the helicase activity (4), we reasoned that the requisite ATPase domain interactions between these gate subunits are critical for helicase activity and that activation by GINS/Cdc45 helps facilitate formation of this structure. How the open and closed conformations of the gate and side channel might come into play during helicase activity has remained unexplored.

Among the several outstanding mechanistic questions with regard to helicase activity and replication fork organization is the path of the lagging strand and the roles, if any, for Cdc45 and GINS in guiding the lagging strand. From the observed positions of these factors and the nexus of the DNA fork junction in EM reconstructions of the complex (18, 20), we reasoned that neither set of factors is positionally capable of serving as a "wedge" that might facilitate unwinding or that might work behind the helicase in a plow-like capacity. Nevertheless, other studies had shown that both Cdc45 (21–23) and the GINS complex (4, 24) have a weak but measurable DNA binding activity. Insofar as the lagging strand would need to exit the central channel following Mcm2–7 activation and DNA melting, it initially seemed possible that this DNA segment might interact with GINS or Cdc45, which could capture it within the side channel created upon closure of the Mcm2/5 gate (18).

To better understand the disposition of DNA segments associated with the CMG, we used protein/nucleic-acid cross-linking methods to define a path for the lagging strand. These studies show that the lagging strand template DNA when bound to the CMG in its translocation mode does not make intimate contact with either Cdc45 or the GINS but that it instead interacts with the MCMs. We refer to this template DNA as "lagging strand" throughout the text. Moreover, we found that in the apo state, the leading strand template DNA cross-links to Cdc45. We refer to this template DNA as "leading strand." Using site-specific mutations directed to residues in the set of β-hairpin elements that project into the central channel of Mcm2–7 (25) [the so-called "pre-Sensor I" (PS1) motifs], we show that the nucleotide dependency of Cdc45 leading strand cross-links is altered, such that Cdc45–DNA contacts form even when ATP is present. Using a recent, higher resolution EM structure of the CMG bound to a tailed DNA substrate (20), along with homology modeling to prokaryotic orthologs of Cdc45, we identify residues within Cdc45 that ablate cross-linking; surprisingly, these alterations also affect helicase activity. Collectively, these data suggest that the gate between Mcm2 and Mcm5 can open at given points and that on these occasions the leading strand may dissociate from the central channel; in such instances, the side channel formed by GINS and Cdc45 would help prevent CMG dissociation and enable re-establishment of productive translocation. Together, our data underscore a potential role for Cdc45 in maintaining contacts with both the leading and lagging strands when the helicase may be stalled—such as during S-phase stress—and where the open gate conformation may persist, a point emphasized by the homology of Cdc45 to the prokaryotic repair protein RecJ (21, 26).

Results

CMG Orientation and Activity on Forked DNA with Fluorescent Probes. We used a variety of fluorescently labeled fork substrates to ask specific questions about the interactions of CMG proteins and used DNA–protein cross-linking to probe interactions either with leading or lagging strands. A table of such substrates is given in Table S1 (all substrates are given numbers by way of cross-referencing with the table). In all figures, the positions where the cross-linkable fluorescein-conjugated thymidines (Ts) reside are represented by green dots, and the base positions for the distance from the dsDNA–ssDNA junction are indicated with numbers. In previous studies, we and others often used Y-fork constructs with ∼40 bases of poly-T on both the 3′ and 5′ unpaired extensions, followed by ∼50 base pairs of duplex DNA (4, 27–29). It is known that DNA sequence may influence binding and poly-pyrimidine stretches frequently have high affinity for helicases (29). We therefore had reason to suspect that a mixed orientation of the CMG bound to our standard substrate might be possible: one with the CMG positioned in a translocation mode moving toward the duplex (3′–5′) and another on the opposite strand, moving away. In Fig. 1*A*, only one strand extends from the duplex, but the lone single-stranded DNA tail appended to each of the two substrates is of opposing polarity. Each single-stranded region contained fluorescein-conjugated Ts on the 3′ arm at base positions –3, –6, –9, and –15 away from the ssDNA–dsDNA junction. Binding affinities were determined by an electrophoretic mobility-shift assay (EMSA), which showed that the CMG has similar K_ds for each substrate, in agreement with our previously published data (4). However, this study also led to the concern that on a fork, we might encounter a confounding combination of cross-linking patterns. We thus tested the possibility suggested by these results that two CMG complexes might engage a fork with poly-T tails oriented in opposite directions. At higher concentrations of the CMG, two shifted bands were detected, whereas at the highest levels of substrate 4 (with only one T-rich arm and a GC-rich arm), only one shifted band was detected (Fig. 1*B*). Forks with G-rich sequences on both single-stranded arms did not form detectable CMG·protein complexes (Fig. 1*C*, lanes 13–20).

We also used a helicase activity assay to ask whether forks bearing fluorescent tags interfered with enzyme function. In these experiments, the CMG was allowed to bind to substrates in the presence of ATPγS, and side-by-side with this binding-only reaction, an excess of ATP was added to allow for unwinding. Fig. 1*C* shows that when the orientation of the T-rich strand is correct to allow unwinding (i.e., so that the CMG moves toward the duplex), DNA–protein complexes and helicase products were observed. In contrast, when the T-rich strand is placed on the 5′ overhang, a shifted nucleoprotein complex is detected, but no helicase activity is observed (Fig. 1*C*, lane 7). Together, these experiments establish that we can orient a single CMG helicase on a bone fide fork substrate in a unique direction and that the binding with fluorescent probes on either arm does not alter binding affinity or helicase activity.

UV Cross-Linking of CMG to Fluorescein-Conjugated Forked Substrates Reveals Protein–DNA Interactions. With a poly-T–rich leading strand (and a GC-rich lagging strand to enforce leading strand encirclement by the Mcm2–7 motor elements), we next sought to define interactions between either strand to the entirety of the CMG. Many amino acids including aromatic (e.g., tyrosine) and charged residues (e.g., lysine) form covalent bonds with

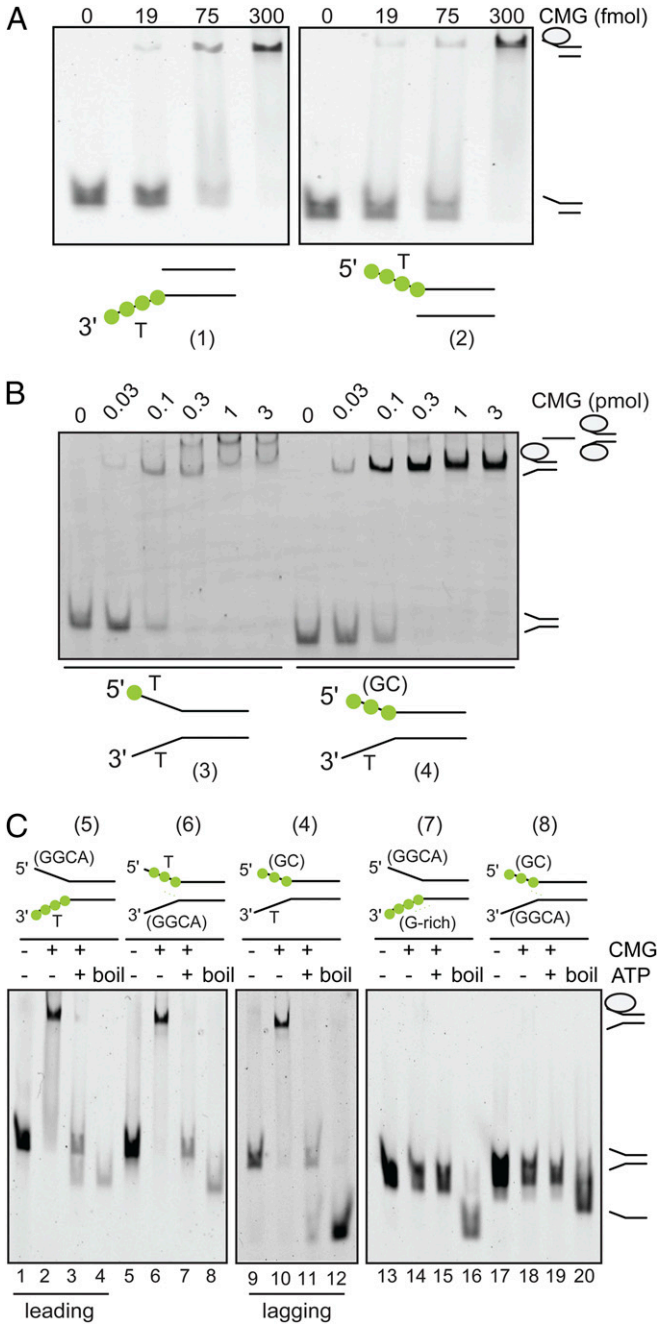

Fig. 1. Poly-T stretches help orient CMG binding to forks with single strands. (*A*) CMG binding to DNA was titrated with fluorescein-labeled DNA substrates (indicated by green dots). The substrates used are diagrammed and have single-strand overhangs from a duplex with poly-T with either a 3′ or 5′ extension. CMG was added to 50 fmol of DNA in a range from 0, 19, 75 and 300 fmol of protein. In this figure and all others, the numbers under the diagrams of the probes refer to Table S1, where the exact sequences are given. (*B*) Indicated amounts of CMG were incubated with 100 fmol of DNA substrates with 3′+5′ extensions of poly-T tracks ("fork" substrate) or 3′ poly-T+ 5′ GC (leading strand substrate) extensions. The fork substrate displays a second supershifted species in the EMSA, which is not present with the leading strand substrate. Signals were detected by fluorescence, and positions of free forked DNA substrates and CMG-bound substrates are indicated on the side. (*C*) DNA binding and helicase activities of CMG were tested using five forked DNA substrates with different nucleotide sequences on the 3′ and 5′ arms (see Table S1 for DNA sequences). For each substrate, 300 fmol of CMG were bound to 50 fmol of DNA in the presence of ATPγS (lanes 2, 6, 10, 14, and 18). For helicase activity, a 100-fold excess of ATP was added and unwinding was detected (lanes 3, 7, 11, 15, and 19). Positions of free DNA substrates, CMG-bound substrates, and displaced substrates are indicated on the side. Free (no protein, lanes 1, 5, 9, 13, and 17) and "boiled" substrates (lanes 4, 8, 12, 16, and 20) are shown for each of the used substrates.

pyrimidine bases through a radical intermediate after UV light radiation (30, 31). We used strand-specific, fluorescein-conjugated Ts positioned along an arm of our forked substrates to identify any protein–DNA interactions specific to that strand induced by UV light. Two types of DNA substrates that differ in where the fluorescein-conjugated Ts were positioned were used to probe protein contacts (Fig. 2*A*): By positioning fluorescein-conjugated Ts along either the leading or the lagging strand, we could further distinguish the direct contacts made by the CMG to either of these strands. After binding of the CMG to the appropriate substrate, samples were exposed to UV light, treated with nuclease (*Materials and Methods*), and individual proteins were separated by SDS/PAGE. The nucleotides transferred to specific proteins were visualized by Western protocols using reagents specific to the fluorescent nucleotide, whereas overlay of the Western blot with the membrane following gold staining identified proteins in the CMG. For simplicity, we will refer to the DNA substrate that contains the fluorescein groups along the 3′ extension as the leading strand substrate and the one with groups along the 5′ extension as the lagging strand substrate (Fig. 2*A*).

For the lagging strand substrate, we designed a substrate with a short 5′ poly-GC overhang (16 nt) or with a GC-rich 40-base overhang (Fig. 2*A*). The CMG was then incubated in the presence or absence of ATPγS with the leading or the lagging strand substrates (Fig. 2*B*). This experimental setup allowed for analysis of the DNA–protein contacts when the Mcm2/5 gate in the Mcm2–7 ring was expected to be open (–ATPγS) or closed (+ATPγS) (20). Strong cross-links were observed at molecular weights comigrating with the Mcm2–7 proteins (Fig. 2*B* and Fig. S1), and the pattern of cross-linking proved distinct for the lagging strand and the leading strand probes. In general, leading strand probes provided stronger signals, implying a more intimate set of CMG contacts—likely occurring within the internal channel of the Mcm2–7 hexamer—than those that were made with the lagging strand. We do note that cross-linking efficiency will also be a function of the specific chemistry afforded by the amino acid residues that are within the appropriate distances from the labeled deoxythymidine residue. Thus, the cross-linking results showed not only a change in the MCM patterns but also an increase in intensity of the cross-links formed when ATPγS was present. Because the detection of cross-linking bands by Western blot induces a slight fuzziness to the bands and because some of the Mcm2–7 protein bands run close or even on top of each other when analyzed by SDS/PAGE, we attempted to better distinguish the signals with the leading strand and confirm the described change in cross-linking pattern by improving the separation between MCM subunits. For this purpose, we engineered a CMG complex that contains MBP-tagged Mcm3 and mCherry-tagged Mcm5 subunits (Fig. 2*D*). Using this construct shows clear separation of all Mcm2–7 proteins and confirms that there is a change in cross-linking in the absence and presence of a nucleotide. For this purpose, we overlay the emission signals at 605 nm for the SYPRO-stained protein with the 520-nm exposed image for highlighting cross-linked fluorescein–nucleotide/protein species. It should be noted that with the protein–DNA bands, there is a slight shift in mobility observed for particular subunits, which might indicate that nuclease digestion was not complete for Mcm5, 6, and 7. Nonetheless, in the case of the lagging strand substrate, the overlay shows that only Mcm5 of the Mcm2–7 complex cross-links to the DNA without the nucleotide and that a switch to other subunits becomes observed only after the nucleotide is bound (Fig. 2*E*).

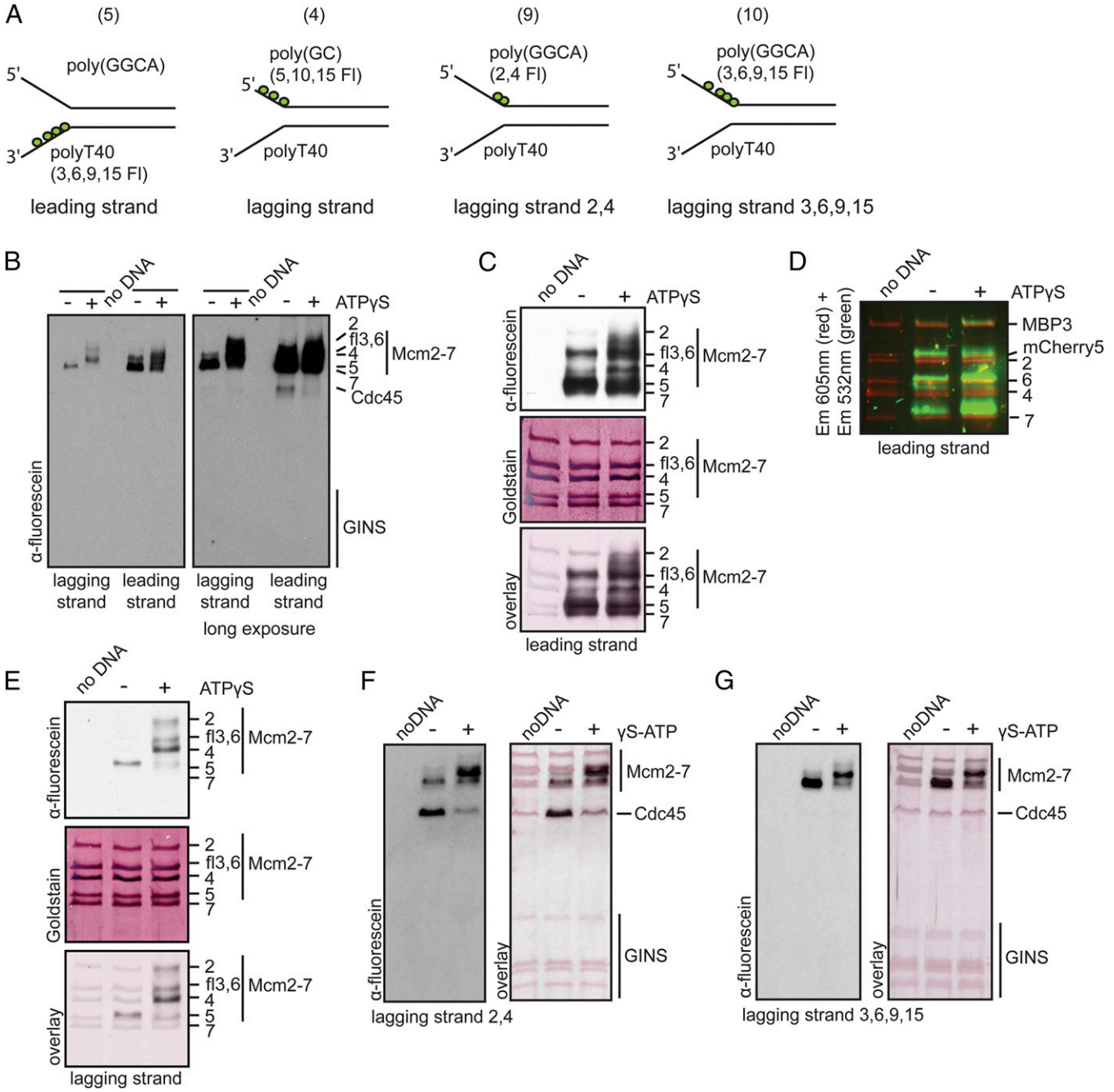

Fig. 2. Cdc45 in the CMG contacts single strands of a fork only in the APO state. (*A*) Schematic for leading and lagging strand DNA substrates used in UV-induced cross-linking assays. The sequence composition of the two single-strand arms and the position of the fluorescein-conjugated nucleotides (green dots) are indicated, and sequences are provided in Table S1. (*B*, *Left*) Immunoblot of leading and lagging DNA substrates cross-linked to wild-type CMG in the absence and presence of ATPγS. We used 200 fmol of protein and 200 fmol of DNA. After UV cross-linking and nuclease digestion as described, proteins were separated by SDS/PAGE (10%) and transferred to support for Western blotting. The immunoblot was probed with monoclonal α-fluorescein antibody to detect cross-linked nucleotide–protein bands. The long exposure (*Right*, ∼6× longer than short exposure) shows that Cdc45 cross-links to the leading strand substrate in the absence of ATPγS. GINS proteins do not cross-link to either substrate. Protein bands were assigned by alignment to the SYPRO red-stained membrane as shown in Fig. S2*A*. (*C*, *Top*) Mcm2–7 part of the immunoblot when the leading strand DNA substrate is cross-linked to wild-type CMG. (*Middle*) The positions of all Mcm2–7 proteins are indicated on the side and were aligned to the gold-stained membrane, to which the proteins were transferred. (*Bottom*) Protein bands were identified by overlay of the Western signal onto the gold-stained membrane. In this and subsequent panels, proteins were separated by SDS/PAGE (8%). (*D*) Mcm2–7 part of the SDS/PAGE (8%) when the leading strand DNA substrate is cross-linked to wild-type CMG with MBP–Mcm3 and mCherry–Mcm5. Overlay of emission signals from SYPRO red-stained protein bands at 605 nm (red) and at 532 nm to visualize the fluorescein–nucleotide:protein bands (green) is shown. (*E*) Mcm2–7 part of the immunoblot when the lagging strand DNA substrate is cross-linked to wild-type CMG (*Top*). Same arrangement as shown under *C*. (*F*) Immunoblot shows proteins of the wild-type CMG, to which nucleotides were cross-linked using the lagging strand 2,4 DNA substrate. Overlay of gold-stained protein bands and Western blot signals of the nucleotide–protein bands is shown on the right. We used 400 fmol of protein and 400 fmol of fork DNA. (*G*) Immunoblot shows proteins of the wild-type CMG, to which nucleotides were cross-linked using the lagging strand 3,6,9,15 DNA substrate. We used 400 fmol of protein and 400 fmol of DNA. Overlay of gold-stained protein bands and Western blot signals of the nucleotide–protein bands is shown on the right. No significant cross-linking of Cdc45 above the background level is observed.

In addition to the expected Mcm2–7 cross-links, upon longer exposures of our Western blots, we unexpectedly found that Cdc45 could also cross-link to the leading strand DNA. This interaction was readily detected in the absence of ATPγS but disappeared in the presence of the nucleotide (Fig. 2*B*, "long exposure"). No interaction was evident between Cdc45 and the lagging strand when positions –5, –10, and –15 bases away from the ss/dsDNA junction were marked with fluorescent Ts (Fig. 2*B*). Moreover, none of the GINS proteins cross-linked to either DNA strand with or without a nucleotide, indicating that there are no direct contacts of this four-protein complex with either the lagging or leading strands in the context of CMG.

Recent EM-based findings from our groups have found that in the presence of a nucleotide, the duplex DNA of the forked substrate lies proximal near Mcm5 at the C terminus of the Mcm2–7 motor (20). This configuration accords with prior findings by others (10, 11, 32), indicating that during separation, both strands are kept in close proximity to the "2/5" gate, with the leading strand entering into the central MCM channel and the lagging strand excluded from the interior of the helicase ring. Given that Cdc45 is situated adjacent to the Mcm2/5 gate, the position of the duplex seen by EM suggested that Cdc45 might also interact with the lagging strand and that probes residing close to the nexus of the ssDNA–dsDNA junction might capture such a contact. To test this idea, we therefore designed a lagging strand substrate with a 5′ 40-nt overhang and positioned the fluorescein groups at positions –2 and –4 bases away from the junction (Fig. 2 *A* and *F* and Fig. S1*B*). Upon cross-linking, a direct interaction of Cdc45 and the junction became apparent in the absence of a nucleotide, and this interaction was greatly diminished when a nucleotide was added (Fig. 2*F*). Further analysis of a lagging strand substrate bearing four fluorescent tags at positions –3, –6, –9, and –15, along with a similar substrate containing only one tag at position 3, showed no cross-linking of the 5′ strand to Cdc45 (Fig. 2*G* and Fig. S1 *C* and *D*). Collectively, these findings indicate that the physical cutoff for the direct interaction of Cdc45 with the lagging strand in the absence of a nucleotide occurs at a point just two bases away from the ssDNA/dsDNA junction and that without nucleotide both the leading strand and the lagging strand bases immediately adjacent to the fork junction interact with Cdc45. Our data also argue that, contrary to prior suggestions (4), the lagging strand is unlikely to be perpetually guided past GINS or Cdc45 during translocation.

Central Core Residues of Mcm2–7 Affect Cdc45–DNA Cross-Linking. Because the interaction of Cdc45 with distal leading strand regions proved dependent upon nucleotides, this finding immediately suggested that the equilibrium between an open and closed conformation of the Mcm2/5 gate might serve as a controlling factor in allowing such interactions. Nucleotide binding is known to help promote closing of the Mcm2/5 gate in the context of the CMG (18) and thus would be expected to favor a translocation mode in which the leading strand runs through the Mcm2–7 central channel. Along these lines, the strong interactions with the leading strand within the central channel might in turn also help favor a closed gate conformation. To test this idea, we introduced mutations in the Mcm2–7 subunits that impair DNA binding by the CMG helicase by lowering the affinity of the Mcm2–7 complex for nucleic acid substrates. The CMG mutant complex we used introduces an alanine substitution for a conserved lysine in the MCM PS1 β-hairpin motif (Fig. S2*A*), an AAA+ ATPase motif previously implicated in DNA binding by both MCMs and superfamily III helicases (33–35). Mutation of the PS1 lysine in archaeal MCMs not only decreases DNA binding but also abolishes helicase activity entirely, suggesting that it plays a pivotal role in coupling ATP turnover to translocation along DNA (35). In *Saccharomyces cerevisiae*, this residue is essential for viability (36).

Mutation of the PS1 lysine in all six Mcm2–7 subunits (named "6xPS1" CMG) did not disrupt the formation of a stoichiometric CMG complex (Fig. S2*C*). However, the DNA binding affinity of the 6xPS1 CMG complex was greatly diminished (Fig. 3*A*). DNA unwinding activity was similarly compromised, with the mutant helicase exhibiting <10% activity of the native CMG (Fig. 3*B*). Next, we analyzed the contacts between 6xPS1 CMG subunits and both the leading and lagging strands of a bound DNA substrate using the cross-linking approach described for wild-type protein. As anticipated from the loss of affinity of the CMG to the fork, and in contrast to the effects seen for Cdc45 cross-linking, the PS1 β-hairpin mutant complex showed significantly reduced cross-linking to the MCMs (to about 20–30% of wild type) with our panel of substrates (Fig. 3*C*, *Upper*). Significantly, however, the cross-linking of the Cdc45 subunit to the leading strand was actually enhanced with this mutant CMG (Fig. 3*C*, *Bottom*). This finding indicates that, even though weakened, DNA binding to the CMG can transiently occur and that the Mcm2/5 gate may open more frequently when interactions between DNA and the Mcm2–7 pore are not at their full potential. Moreover, a comparable level of Cdc45–DNA cross-linking was also detected in the 6xPS1 mutant even when a nucleotide was present (Fig. 3*C* and Fig. S2*E*), again suggesting that impaired leading strand DNA binding within the MCM interior can reciprocally lead the leading strand to slip through the gate and encounter Cdc45. Nucleotide-independent cross-linking to the lagging strand 2,4 substrate was similarly observed with the 6xPS1 mutant (Fig. 3*D* and Fig. S2*F*), indicating that it is not just the leading strand that can slip out but the entirety of the fork junction.

The Lagging Strand Touches the Mcm2–7 External Surface. The clear cross-talk between nucleotide-dependent DNA binding by both the Mcm2–7 subunits and Cdc45 within the CMG prompted us to probe further the contacts of the lagging strand within the complex. Studies in Archaea and in *Xenopus* have indicated that the lagging strand is excluded from the MCM central channel and may follow a path around the exterior surface of the ring (10, 11, 37). When using DNA substrates that can be unwound, the lagging strand was not observed to interact with GINS/Cdc45 of the CMG, but cross-linking to the MCMs was detected (Fig. 2*B*).

To examine prospective lagging strand interactions more closely, lysine residues within a second conserved β-hairpin motif, albeit one that is located on the exterior MCM surface (11, 32), were mutated to alanine in all six Mcm2–7 subunits (Fig. S2*B*). After purifying this mutant CMG complex (termed "6xEXT") (Fig. S2*D*), we analyzed its interactions and activity on DNA. Only a minor decrease in DNA binding by the 6xEXT CMG was observed in EMSA studies (~80% of wild type), but DNA unwinding was substantially reduced compared with the wild-type CMG (<5%) (Fig. 3*E*). Cross-linking interactions between the 6xEXT CMG and the leading strand DNA probes showed no discernable differences with the wild-type CMG, indicating that these motifs do not affect internal channel protein/DNA interactions (Fig. 3*F*, *Middle* and Fig. S2*G*). Interestingly, no interactions between Cdc45 or GINS and the lagging strand were observed with the 6xEXT complex as seen with the wild-type CMG, and DNA–protein interactions between the lagging strand and MCM proteins were likewise diminished with the mutant complex (Fig. 3*F*, *Top* and Fig. S2*G*). These findings are consistent with the idea that, as proposed for the archaeal MCMs (11), the lagging strand is likely guided around the external surface of Mcm2–7 in the context of the CMG.

For the wild-type CMG in the absence of a nucleotide, only Mcm5 can been seen to lie proximal to the lagging strand, suggesting that this DNA segment prefers to reside near the Mcm2/5 gate (Fig. 3*F*). Upon addition of ATPγS, however, the cross-linking pattern to the native CMG switches primarily to

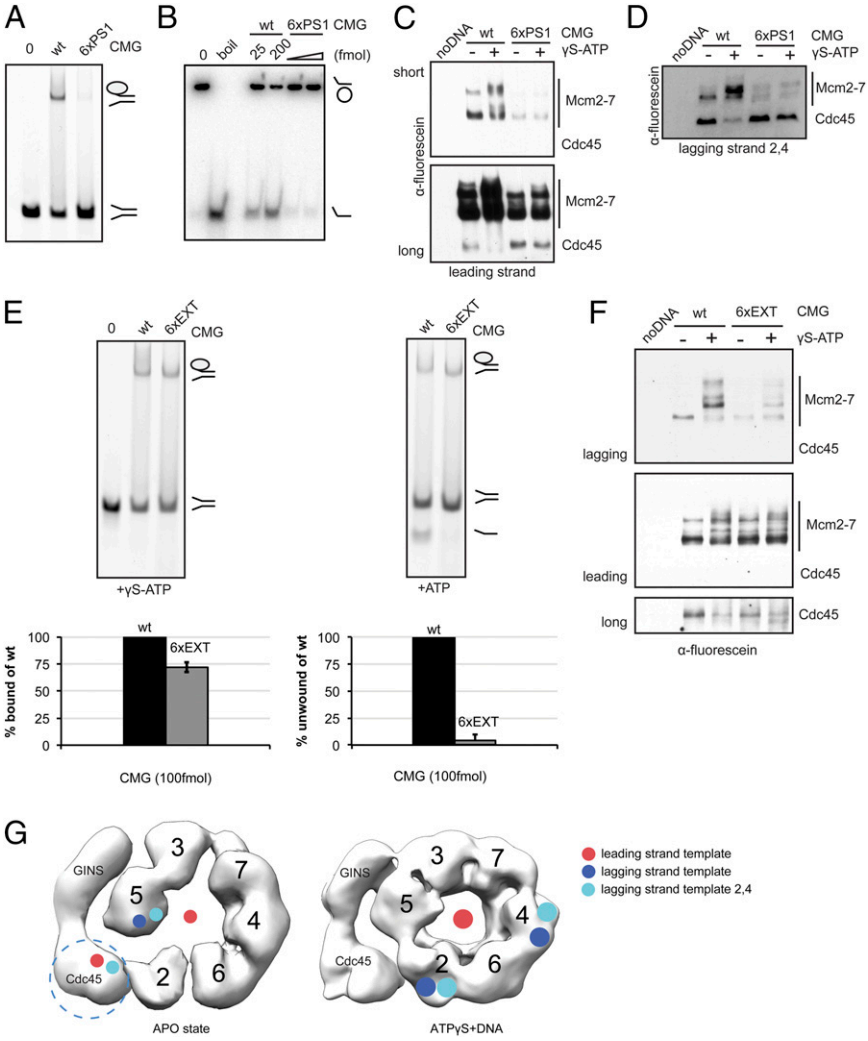

Fig. 3. Mutations in Mcm2–7 affect the DNA contacts of Cdc45 in the CMG complex. (*A*) EMSA of wild-type CMG and CMG complex with mutations in the PS1 β-hairpin of all six Mcm2–7 proteins (named 6xPS1). "0" shows the control lane without protein. All lanes contained 100 fmol of fluorescein-labeled forked DNA substrate (3′+5′ poly-T, fork) and where indicated 100 fmol of purified CMG protein in the presence of 10 μM of ATPγS. Reactions were separated on a native TBE (Tris/Borate/EDTA) polyacrylamide gel (4%). Positions of free and CMG-bound substrates are indicated on the side. (*B*) Helicase activity assays. Positions of circular substrate and the single-strand oligonucleotide released from the M13 are indicated on the side. Two concentrations of CMG (25 and 200 fmol) were added to 1 fmol of radiolabeled substrate and 300 μM of ATP. Products were separated by TBE–PAGE (8%). 0 and boil are substrate controls without protein or with boiled substrate, respectively, and an autoradiogram of the reaction products is shown. (*C*) Immunoblot shows proteins of the 6xPS1–CMG complex that were cross-linked to the leading strand substrate under UV and treated with nuclease as described. Proteins were separated by SDS/PAGE (8%). Short (*Top*) and long (*Bottom*, ∼6 times longer) exposure times are shown. (*D*) Immunoblot shows proteins of the 6xPS1 CMG complex that were cross-linked to the lagging strand 2,4 DNA substrate. Reaction products were separated by SDS/PAGE (10%). (*E*, *Left*) EMSA with wild-type CMG and 6xEXT CMG complex. 0 shows the control lane without protein. All reactions had 100 fmol of leading strand substrate and 100 fmol of purified CMG protein in the presence of 10 μM of ATPγS. (*Right*) Helicase activity assay with leading strand substrate. After initial binding of CMG to DNA in the presence of 10 μM of ATPγS, unwinding was initiated by addition of 300 μM of ATP. Positions of free DNA and displaced strand are shown on the right. Quantifications of two independent series of both EMSA and helicase activity assay are shown below. (*F*) Immunoblot shows proteins of the 6xEXT–CMG complex that were cross-linked to the leading and lagging strand substrates. Reaction products were separated by SDS/PAGE (8%). For the leading strand, a longer exposure is shown on the bottom to visualize Cdc45. (*G*) Summary of the cross-linking results with various DNA substrates in the apo and ATPγS-bound states of CMG (subunits of complex are identified). The different substrates are color coded and listed below. The change from small to large circles indicates a switch from a cross-linking signal with the different conditions of the assays. In the apo state, Cdc45 cross-links to the leading strand, whereas to the lagging strand only right at the ssDNA–dsDNA junction. When a nucleotide is bound, the Mcm2–7 proteins cross-link to the leading strand substrate likely through the central channel, whereas the interactions with the lagging strand must reside on the exterior surface.

Mcm4, with weaker cross-linking also seen for several other subunits, such as Mcm2. These data suggest that during wrapping and translocation, the lagging strand slides away from the 2/5 gate and toward Mcm4. Fig. 3*G* summarizes the switches of CMG binding to DNA in the apo and ATPγS states as captured by cross-linking; only those Mcm2–7 subunits that cross-link to DNA probes that could be readily identified and that represented the strongest protein–DNA interactions are highlighted.

Orthology to RecJ Allows Modeling of the Cdc45 Structure and Identification of Critical Residues for Cross-Linking and Helicase Activity. The ability of Cdc45 to cross-link to the leading DNA strand in the apo state was unexpected and suggested to us that Cdc45 might serve a function beyond working with the GINS subcomplex to induce correct contacts between CMG subunits. More specifically, it seemed possible that when the helicase traverses through different translocation or paused states, the

gate between subunits Mcm2 and 5 might occasionally open, allowing the accidental escape of the leading strand from the central channel. In this vein, the vestibule provided by Cdc45 and GINS, and the DNA binding properties of Cdc45 in particular, might in turn serve to catch the strand and allow for a reestablishment of proper interactions into the central motor.

We were curious as to which region of Cdc45 could participate directly in such interactions and used the structural data provided by Costa et al. (2014) (20), along with sequence alignments to ask this question. Fold and function assignment system (FFAS)03 searches (38) have identified strong sequence conservation between the catalytic domain of RecJ, a bacterial exonuclease, and the N terminus of the Cdc45 proteins (21, 26). We also found good sequence agreement between a related protein, an exopolyphosphatase, and both Cdc45 and RecJ. These similarities allowed us to generate two independent homology models for the *N* and C lobes of Cdc45 based on the *Thermus thermophilus* RecJ crystal structure [Protein Data Bank (PDB) ID code 1ir6] (Fig. 4*A*, magenta) and the RecJ-related exopolyphosphatase protein (PDB ID code 2qb6) (Fig. 4*A*, cyan).

Based on the known DNA binding regions of these proteins, the resultant structural information was next used to predict how the corresponding region of Cdc45 would fit together with the rest of the CMG (20) and which of its residues might in turn interact with a client leading strand substrate. This exercise highlighted two conserved candidate residues, K363 and R419 (Fig. 4*A*, highlighted in red); R419 in particular resides in a conserved Lys-Ser-Arg motif (Fig. 5*A*), as is shown in the alignment of Cdc45 sequences from different metazoans (*Homo sapiens*, *Xenopus laevis*, *M. musculus*, and *Drosophila melanogaster*) (Fig. 4*B*).

To test the role of the conserved basic residues in Cdc45, we made CMG complexes containing either single (K363A or R419A) or double (K363A+R419A, "2x") mutations and tested their activities biochemically (Fig. S3*A*). As shown in Fig. 4*C*, all three CMG complexes bearing a mutant Cdc45 subunit displayed wild-type DNA binding in EMSAs. Furthermore, the on-rates of these mutant CMG complexes were as rapid as the wild-type complex, suggesting that these mutations do not affect the loading of the leading strand into the central Mcm2–7 core (Fig. S3*B*). However, cross-linking between Cdc45 and DNA in the absence of a nucleotide was abolished for both the double mutant 2x and R419A CMG complexes with both leading and lagging strand probes (Fig. 4 *D* and *E*). These data show that R419 of *Drosophila* Cdc45 is essential for the direct DNA interactions observed for this subunit in our cross-linking assays.

To further examine the consequences of the Cdc45 R419A mutation, we examined its effects on cross-linking between DNA and the Mcm2–7 subunits. In contrast to the outcome on Cdc45, no loss of interactions with the MCMs was detected (Fig. 4*D*, *Top*). Furthermore, the helicase activity of each of the three mutant–Cdc45 CMG complexes was similarly comparable to the native complex (Fig. 4*F* and Fig. S3*C*). Thus, DNA binding by Cdc45 does not appear important for the unwinding of short

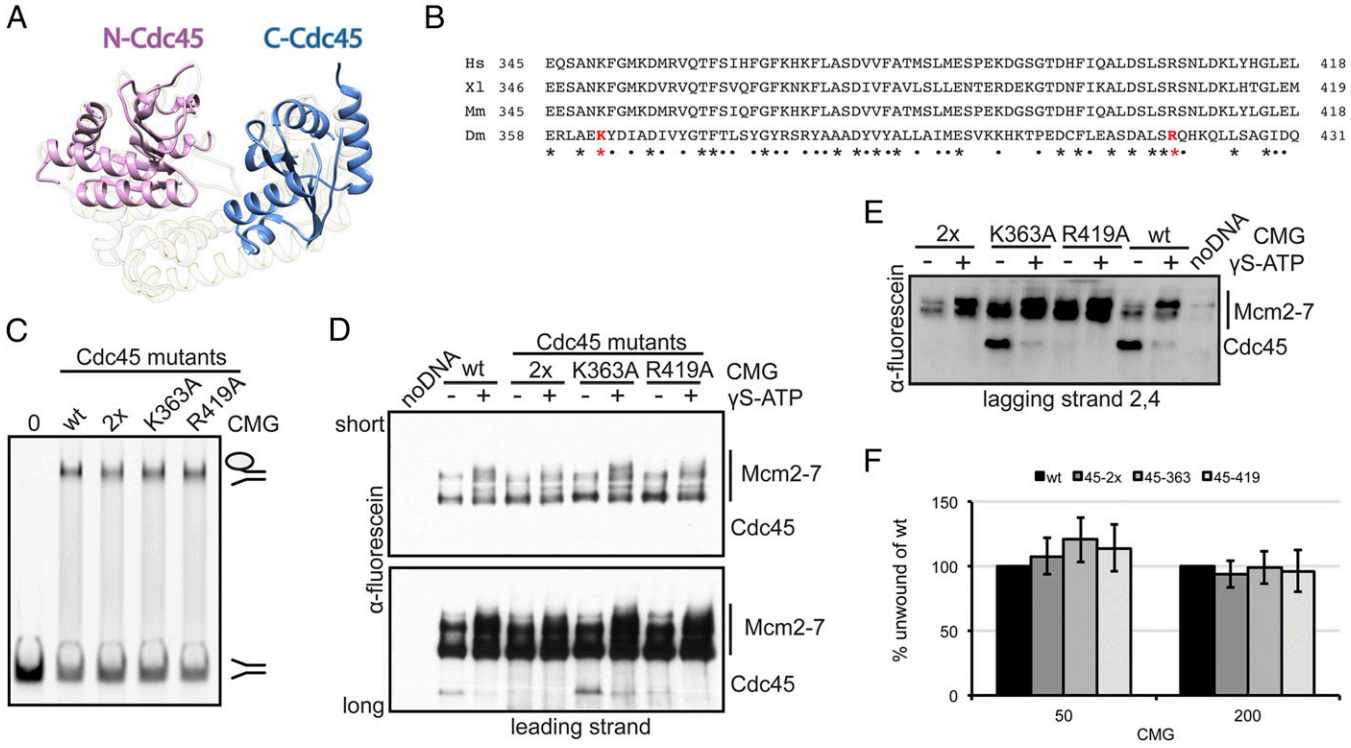

Fig. 4. Specific Cdc45 residues contact the leading strand within the CMG complex. (*A*) Ribbon representation of the *N*- and C-terminal Cdc45 homology models. The *T. thermophilus* RecJ–exonuclease scaffold is shown as transparent with the C-terminal lobe of Cdc45 modeled in cyan above the silhouetted ribbon. The *N*-terminal domain of Cdc45 is shown in magenta. (*B*) Sequence alignment of Cdc45 proteins in the domain containing the two putative DNA binding residues K363 and R419 (red). Asterisks show conserved residues and dots similar residues: *H. sapiens*, *X. laevis*, *M. musculus*, and *D. melanogaster*. (*C*) EMSA comparing wild-type and Cdc45–mutant CMG complexes. 0 shows a control lane with substrate alone; all other lanes show 100 fmol of 3′+5′ poly-T fork with 100 fmol of CMG protein in the presence of 10 μM of ATPγS. 2x indicates mutant complexes harboring alanine substitution changes in place of K363 and R419. DNA·protein complexes were separated from the duplex on a native TBE gel (4%). (*D*) Immunoblot shows proteins of CMG complexes (200 fmol) with mutations in Cdc45 that were cross-linked to the leading strand DNA substrate (200 fmol). The long exposure is shown on the bottom to visualize Cdc45. (*E*) Immunoblot of cross-linked CMG proteins with mutations in Cdc45 (400 fmol) to the lagging strand 2,4 DNA substrate (400 fmol). (*F*) Quantification of CMG helicase activity assay on a circular DNA substrate. Two protein amounts (50 and 200 fmol) were assayed, and average values with SDs for six independent series are given.

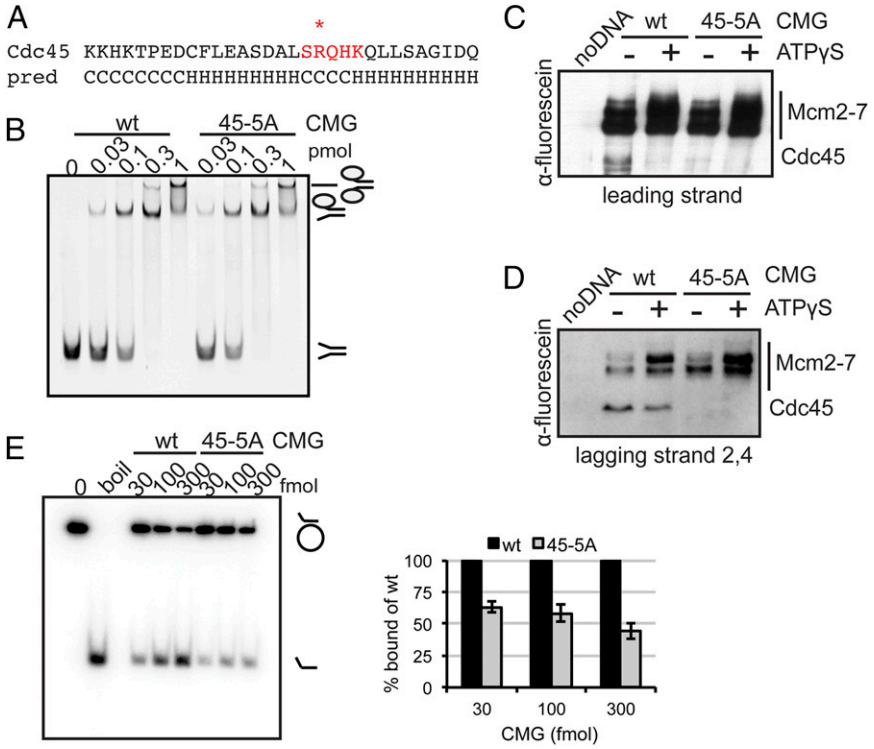

Fig. 5. Cdc45 loop affects the helicase activity of CMG. (*A*) The helix-loop-helix motif, in which R419 is embedded in DmCdc45. All residues highlighted in red were changed to alanine (5A mutant). (*B*) EMSA assay of a protein titration of wild-type and Cdc45 loop mutant (5A) CMG. 0 shows the control lane with substrate alone, and all other lanes contain 100 fmol of 3′+5′ poly-T fork with 100 fmol of CMG with 10 μM of ATPγS. Reaction products were separated on a native TBE gel (5%). (*C*) Immunoblot shows proteins of wild-type and Cdc45-5A mutant CMG complexes (200 fmol) that were cross-linked to the leading strand DNA substrate (200 fmol). The long exposure is shown on the bottom. (*D*) Immunoblot of cross-linked wild-type and Cdc45-5A mutant CMG complexes (400 fmol) to the lagging strand 2,4 DNA substrate (400 fmol). (*E*) Helicase activity assay on a circular DNA substrate titrating CMG proteins (30, 100, and 300 fmol) in the presence of 300 μM of ATP. Reaction products were separated by TBE–PAGE (8%). Quantification of the helicase activity is shown below with average values and SD from two independent series.

duplexes in the context of the CMG, indicating that this subunit does not serve as a primary driver of fork separation.

To probe the role of the LSR region of Cdc45 in more detail, we next proceeded to purify a mutant CMG complex in which five resident amino acids, predicted to be in a loop (Ser418–His421), were changed to alanine (Fig. 5*A* and Fig. S4*A*). The DNA binding affinity of this mutant ("45-5A-CMG") was unchanged compared with the wild-type CMG in quantitative EMSA assays (Fig. 5*B*). As anticipated from the cross-linking data with the single R419A mutant, the quintuple Cdc45 mutant (45-5A-CMG) did not cross-link to the leading or lagging strand substrates in either nucleotide state (Fig. 5 *C* and *D* and Fig. S4 *B* and *C*). In comparing the helicase activities of the wild-type CMG and the 45-5A-CMG mutant on a circular ssDNA substrate containing an annealed 50-base-pair complementary strand (Fig. 5*E*), we found that complete substitution of the LSR loop diminished unwinding by approximately twofold (Fig. 5*E*), again indicating DNA binding by Cdc45 is not critical for central duplex unwinding activity of Mcm2–7 within the CMG.

Discussion

The role of Cdc45 in replisome function has been enigmatic. Earlier studies initially focused on how Cdc45 would participate with GINS in activating the helicase at the licensed ori site. In previous work, we had found that free Mcm2–7 complexes primarily adopt an open lock washer conformation (18, 39). Our proposal is that Cdt1 binding, a molecular matchmaker that brings the Mcm2–7 hexamers to the ori-bound ORC, may topologically seal off the Mcm2–5 gate, inducing the formation of a more planar ring state observed by others (40). Thus, the roles for ORC and Cdc6 in MCM loading would involve helping to release Cdt1 from an ori-tethered hexamer, after which the complex would revert to an open gate state competent to subsequently engage duplex DNA (18). ATPase activity has been shown to be important for helicase loading (41, 42). Elegant studies of the licensing reaction by Speck and colleagues have substantially validated the role of the Mcm2/5 gate in this step toward initiation (43).

Our initial EM model for the CMG suggested that Mcm2–7 activation might also require a gating function between the Mcm2/5 subunits, whereby a melted single strand would exit the central pore and be captured by an external compartment formed between GINS, Cdc45, and the lateral edge of the MCM ring (18). Others studying isolated Cdc45 have resurrected the idea that Cdc45 may act as a wedge to split the duplex apart (22). The cross-linking studies presented here were initiated to ask if the lagging strand moves through the external channel formed by the association of GINS and Cdc45 with the Mcm2–7 proteins (18). Significantly, our data provide evidence against both of these models and instead suggest a new role for Cdc45, that of a "guardian" of the gate, which may capture an errant leading strand that happens to escape from the Mcm2–7 motor.

The data here suggest that the special gating function of Mcm2 and 5 presents an "Achilles heel" for the helicase on DNA. The side compartment bounded by GINS and Cdc45 may have evolved in part to solve this problem. Once the appropriate architectural organization has been established for an active helicase, the leading strand needs to remain fully engaged within the Mcm2–7 ring. Accidental sliding or slipping off of the DNA from the pore would have detrimental consequences in the

absence of such a capture mechanism. A tight interaction with the leading strand mediated internally is thermodynamically favored and is substantiated by experiments performed with mutant CMG complexes containing single alanine substitutions in the PS1 β-hairpin. These data show a weakened DNA binding affinity. In such mutants, cross-linking to Cdc45 was detected even with a nucleotide bound to the MCMs, and the effects of the Cdc45-5A mutation upon helicase activity imply that the gatekeeper function for Cdc45 is important. The Mcm2–7 ring within the active CMG, as in all AAA+ complexes, will have a subunit pattern of bound and unbound nucleotide that changes during translocation. Presently, we have no measure of the differences in equilibrium constants between the open and closed states with various nucleotide occupancies. It is possible that when no nucleotide is bound in the translocating helicase, the leading strand might slip out and be guided quickly back into the central channel.

Drosophila Cdc45, along with its eukaryotic counterparts, is a member of the RecJ/DHH exonuclease superfamily. Cdc45 has lost its nuclease activity through amino acid replacements to metal-binding elements in the RecJ catalytic center but has retained an ability to bind single-stranded nucleic acids (21, 22). We propose that in the context of the CMG, this weak DNA binding capability allows for the capture of the leading strand and a fork junction when the Mcm2/5 gate opens, a state that may occur at points of stress, such as when the helicase stalls. To date there is no direct evidence that an APO state occurs in cells; further studies are needed to ask if an open gate state occurs at roadblocks put in front of the fork by damage or if in fact the gate may open periodically upon ADP release after ATP hydrolysis in the Mcm5 subunit during replisome progression. Critically, the interactions determined by our studies require residues in the RecJ-like, single-stranded DNA binding domain of Cdc45. The positioning of the DNA binding domain of Cdc45 within the CMG complex would allow this binding domain to capture the leading strand in a 3′–5′ orientation (Fig. 6) (20). Although bacterial RecJ is a 5′–3′ exonuclease, binding polarities can switch between homologous proteins over the course of evolution; along these lines, in the archaeal organism *Pyrococcus furiosus*, the RecJ/Cdc45 homolog has been reported to be a 3′–5′ exonuclease (44). Given that the archaeal RecJ homologs of Cdc45 associate with GINS (45, 46), it will be informative to understand in more depth how the repair and replication functions of these proteins are coordinated.

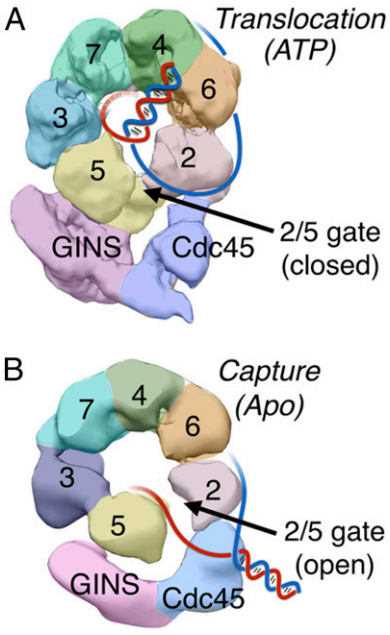

Fig. 6. Model. Shown are AAA+ views of the CMG–EM (*A*) in the presence of ATPγS ("Translocation") where the model used here are the volumes shown in Costa et al. (2014) (20) and (*B*) in the absence of nucleotide ("Capture") with the model from Costa et al. (2011) (18). The leading and the lagging strands are color coded with red and blue, respectively. The model and data that support the depicted switch in DNA strand placements are derived from cross-linking and mutational data as well as structural considerations as discussed in the text.

The notion that Cdc45 plays a role when the helicase encounters a stall is also compatible with other studies that have focused on a repair function for Cdc45 in eukaryotes. For example, Hashimoto et al. have reported that the GINS complex dissociates from the CMG in *Xenopus* extracts after the helicase pauses upon encountering a double-strand break and that retention of Cdc45 with MCMs on DNA is critical for restarting DNA replication after repair (47). Retaining Cdc45 during stalling could help prevent Mcm2–7 from fully losing its local association with DNA and provide a means for the leading strand to reenter and engage the Mcm2–7 pore during replication restart. Along similar lines, biochemical studies of budding yeast Cdc45 found that two single point mutations in the homologous putative LSR loop region of ScCdc45 had very minor effects on single-strand DNA binding. However, when these mutations were combined with two other mutations more distal to the loop, Cdc45 lost single-strand DNA binding (23). Cells containing this quadruple mutant Cdc45 in turn became more sensitive to hydroxyurea stress than the wild-type strain. Bruck and Kaplan (23) hypothesize that the Cdc45–ssDNA interaction might play a crucial role during stalling of DNA polymerase and that this may lead to uncoupling of polymerase from the helicase.

The paths of the single strands shown in Fig. 6 *A* and *B* account for all of the cross-linking data depicted in Fig. 3*G*. In this figure, the 3′ leading strand is red and the 5′ lagging strand is blue. In Fig. 6*A*, the closed and functional translocation mode is diagrammed, and we show in general terms where the lagging strand might wrap around the external surface of the MCMs as guided by a path defined by the external β-hairpins. The unique direction of the lagging strand around this path is suggested by cross-linking data, where only some of the subunits cross-link to the lagging strand (Fig. 2*F*), and by the relative order of the Mcm2–7 subunits. Our cross-linking and functional data are also consistent with work from archaeal MCM proteins, which have shown that these helicases also engage the 5′ lagging strand around the exterior (11–13, 35, 48), and with both biochemical and structural data showing that the 5′ end of a leading strand bound by Mcm2–7 resides near the C-terminal AAA+ ATPase domains of the motor (12, 20).

In considering the Cdc45 "gate guardian" model, we note that the leading strand cross-links with the majority of the Mcm2–7 subunits when a nucleotide is present, and ascribe such contacts to those made within the central MCM channel. In this vein, Costa et al. (2014) (20) show that for the CMG bound to DNA in the presence of a nucleotide, the single/double-strand junction sits at the AAA+ end of the complex, with the leading and lagging strands proximal to Mcm5. In switching from a translocation state to a fully open gate conformation, we posit that the leading strand may slip out of the central channel, with a large change in DNA positioning required to maintain contact with the helicase. This repositioning in how DNA is bound would allow Cdc45 to capture both the leading strand and the lagging strand region immediately adjacent to the ss–ds fork junction. The salient results that reinforce the model include the finding that only in the open gate configuration does Cdc45 cross-link tightly to the leading single strand. Furthermore, the leading strand cross-links to the CMG when probes are placed at nucleotide positions distal to the fork junction. In contrast, away from the fork junction, we did not detect cross-linking with lagging strand probes. Cross-linking to the lagging strand was only found at the nexus of the fork. Further studies will be needed to ascertain when on an active replisome such a putative

transition from an open gate to a closed conformation might occur; at present, our and others' published data suggest that such a slip might occur upon stalling of the helicase when encountering road blocks or double-strand breaks.

Materials and Methods

Detailed protocols for cloning, protein expression and purification, DNA helicase and EMSA assays, UV-induced cross-linking, and a list of oligonucleotide sequences for DNA substrates can be found in *SI Materials and Methods*.

ACKNOWLEDGMENTS. This work was supported by a PhD fellowship from the Boehringer Ingelheim Fonds (to T.P.), National Research Service Award GM821972 (to J.J.P.), a European Molecular Biology Organization long-term postdoctoral fellowship and Cancer Research UK funding (to A.C.), National Institute of General Medical Sciences Grant GM071747 (to J.M.B.), and National Cancer Institute Grant CA R37-30490 (to M.R.B.).

1. Yardimci H, Walter JC (2014) Prereplication-complex formation: A molecular double take? *Nat Struct Mol Biol* 21(1):20–25.
2. Heller RC, et al. (2011) Eukaryotic origin-dependent DNA replication in vitro reveals sequential action of DDK and S-CDK kinases. *Cell* 146(1):80–91.
3. Moyer SE, Lewis PW, Botchan MR (2006) Isolation of the Cdc45/Mcm2-7/GINS (CMG) complex, a candidate for the eukaryotic DNA replication fork helicase. *Proc Natl Acad Sci USA* 103(27):10236–10241.
4. Ilves I, Petojevic T, Pesavento JJ, Botchan MR (2010) Activation of the MCM2-7 helicase by association with Cdc45 and GINS proteins. *Mol Cell* 37(2):247–258.
5. Aparicio T, Ibarra A, Méndez J (2006) Cdc45-MCM-GINS, a new power player for DNA replication. *Cell Div* 1:18.
6. Pacek M, Tutter AV, Kubota Y, Takisawa H, Walter JC (2006) Localization of MCM2-7, Cdc45, and GINS to the site of DNA unwinding during eukaryotic DNA replication. *Mol Cell* 21(4):581–587.
7. Kang YH, Galal WC, Farina A, Tappin I, Hurwitz J (2012) Properties of the human Cdc45/Mcm2-7/GINS helicase complex and its action with DNA polymerase epsilon in rolling circle DNA synthesis. *Proc Natl Acad Sci USA* 109(16):6042–6047.
8. Remus D, et al. (2009) Concerted loading of Mcm2-7 double hexamers around DNA during DNA replication origin licensing. *Cell* 139(4):719–730.
9. Evrin C, et al. (2009) A double-hexameric MCM2-7 complex is loaded onto origin DNA during licensing of eukaryotic DNA replication. *Proc Natl Acad Sci USA* 106(48): 20240–20245.
10. Fu YV, et al. (2011) Selective bypass of a lagging strand roadblock by the eukaryotic replicative DNA helicase. *Cell* 146(6):931–941.
11. Graham BW, Schauer GD, Leuba SH, Trakselis MA (2011) Steric exclusion and wrapping of the excluded DNA strand occurs along discrete external binding paths during MCM helicase unwinding. *Nucleic Acids Res* 39(15):6585–6595.
12. Rothenberg E, Trakselis MA, Bell SD, Ha T (2007) MCM forked substrate specificity involves dynamic interaction with the 5′-tail. *J Biol Chem* 282(47):34229–34234.
13. Costa A, et al. (2008) Cryo-electron microscopy reveals a novel DNA-binding site on the MCM helicase. *EMBO J* 27(16):2250–2258.
14. Froelich CA, Kang S, Epling LB, Bell SP, Enemark EJ (2014) A conserved MCM single-stranded DNA binding element is essential for replication initiation. *eLife* 3:e01993.
15. Gambus A, et al. (2009) A key role for Ctf4 in coupling the MCM2-7 helicase to DNA polymerase alpha within the eukaryotic replisome. *EMBO J* 28(19):2992–3004.
16. Im JS, et al. (2009) Assembly of the Cdc45-Mcm2-7-GINS complex in human cells requires the Ctf4/And-1, RecQL4, and Mcm10 proteins. *Proc Natl Acad Sci USA* 106(37): 15628–15632.
17. Langston LD, et al. (2014) CMG helicase and DNA polymerase ε form a functional 15-subunit holoenzyme for eukaryotic leading-strand DNA replication. *Proc Natl Acad Sci USA* 111(43):15390–15395.
18. Costa A, et al. (2011) The structural basis for MCM2-7 helicase activation by GINS and Cdc45. *Nat Struct Mol Biol* 18(4):471–477.
19. Bochman ML, Schwacha A (2008) The Mcm2-7 complex has in vitro helicase activity. *Mol Cell* 31(2):287–293.
20. Costa A, et al. (2014) DNA binding polarity, dimerization, and ATPase ring remodeling in the CMG helicase of the eukaryotic replisome. *eLife* 3:e03273.
21. Krastanova I, et al. (2012) Structural and functional insights into the DNA replication factor Cdc45 reveal an evolutionary relationship to the DHH family of phosphoesterases. *J Biol Chem* 287(6):4121–4128.
22. Szambowska A, et al. (2014) DNA binding properties of human Cdc45 suggest a function as molecular wedge for DNA unwinding. *Nucleic Acids Res* 42(4): 2308–2319.
23. Bruck I, Kaplan DL (2013) Cdc45 protein-single-stranded DNA interaction is important for stalling the helicase during replication stress. *J Biol Chem* 288(11):7550–7563.
24. Boskovic J, et al. (2007) Molecular architecture of the human GINS complex. *EMBO Rep* 8(7):678–684.
25. Miller JM, Arachea BT, Epling LB, Enemark EJ (2014) Analysis of the crystal structure of an active MCM hexamer. *eLife* 3:e03433.
26. Sanchez-Pulido L, Ponting CP (2011) Cdc45: The missing RecJ ortholog in eukaryotes? *Bioinformatics* 27(14):1885–1888.
27. Bochman ML, Schwacha A (2007) Differences in the single-stranded DNA binding activities of MCM2-7 and MCM467: MCM2 and MCM5 define a slow ATP-dependent step. *J Biol Chem* 282(46):33795–33804.
28. Lee JK, Hurwitz J (2001) Processive DNA helicase activity of the minichromosome maintenance proteins 4, 6, and 7 complex requires forked DNA structures. *Proc Natl Acad Sci USA* 98(1):54–59.
29. You Z, et al. (2003) Thymine-rich single-stranded DNA activates Mcm4/6/7 helicase on Y-fork and bubble-like substrates. *EMBO J* 22(22):6148–6160.
30. Morimoto S, et al. (1998) Hydroxyl radical-induced cross-linking of thymine and lysine: Identification of the primary structure and mechanism. *Bioorg Med Chem Lett* 8(7): 865–870.
31. Evans MD, Dizdaroglu M, Cooke MS (2004) Oxidative DNA damage and disease: Induction, repair and significance. *Mutat Res* 567(1):1–61.
32. Brewster AS, Slaymaker IM, Afif SA, Chen XS (2010) Mutational analysis of an archaeal minichromosome maintenance protein exterior hairpin reveals critical residues for helicase activity and DNA binding. *BMC Mol Biol* 11:62.
33. Enemark EJ, Joshua-Tor L (2006) Mechanism of DNA translocation in a replicative hexameric helicase. *Nature* 442(7100):270–275.
34. Gai D, Zhao R, Li D, Finkielstein CV, Chen XS (2004) Mechanisms of conformational change for a replicative hexameric helicase of SV40 large tumor antigen. *Cell* 119(1): 47–60.
35. McGeoch AT, Trakselis MA, Laskey RA, Bell SD (2005) Organization of the archaeal MCM complex on DNA and implications for the helicase mechanism. *Nat Struct Mol Biol* 12(9):756–762.
36. Lam SK, et al. (2013) The PS1 hairpin of Mcm3 is essential for viability and for DNA unwinding in vitro. *PLoS ONE* 8(12):e82177.
37. Brewster AS, et al. (2008) Crystal structure of a near-full-length archaeal MCM: Functional insights for an AAA+ hexameric helicase. *Proc Natl Acad Sci USA* 105(51): 20191–20196.
38. Jaroszewski L, Rychlewski L, Li Z, Li W, Godzik A (2005) FFAS03: A server for profile–profile sequence alignments. *Nucleic Acids Res* 33(Web Server issue):W284–W288.
39. Lyubimov AY, Costa A, Bleichert F, Botchan MR, Berger JM (2012) ATP-dependent conformational dynamics underlie the functional asymmetry of the replicative helicase from a minimalist eukaryote. *Proc Natl Acad Sci USA* 109(30):11999–12004.
40. Sun J, et al. (2013) Cryo-EM structure of a helicase loading intermediate containing ORC-Cdc6-Cdt1-MCM2-7 bound to DNA. *Nat Struct Mol Biol* 20(8):944–951.
41. Kang S, Warner MD, Bell SP (2014) Multiple functions for Mcm2-7 ATPase motifs during replication initiation. *Mol Cell* 55(5):655–665.
42. Coster G, Frigola J, Beuron F, Morris EP, Diffley JF (2014) Origin licensing requires ATP binding and hydrolysis by the MCM replicative helicase. *Mol Cell* 55(5):666–677.
43. Sun J, et al. (2014) Structural and mechanistic insights into Mcm2-7 double-hexamer assembly and function. *Genes Dev* 28(20):2291–2303.
44. Yuan H, et al. (2013) RecJ-like protein from Pyrococcus furiosus has 3′-5′ exonuclease activity on RNA: Implications for proofreading of 3′-mismatched RNA primers in DNA replication. *Nucleic Acids Res* 41(11):5817–5826.
45. Marinsek N, et al. (2006) GINS, a central nexus in the archaeal DNA replication fork. *EMBO Rep* 7(5):539–545.
46. Li Z, et al. (2011) A novel DNA nuclease is stimulated by association with the GINS complex. *Nucleic Acids Res* 39(14):6114–6123.
47. Hashimoto Y, Puddu F, Costanzo V (2012) RAD51- and MRE11-dependent reassembly of uncoupled CMG helicase complex at collapsed replication forks. *Nat Struct Mol Biol* 19(1):17–24.
48. Bell SD, Botchan MR (2013) The minichromosome maintenance replicative helicase. *Cold Spring Harb Perspect Biol* 5(11):a012807.